Axiomatix

Marina del Rey ● California

INTEGRATED SOURCE AND CHANNEL
ENCODED DIGITAL COMMUNICATION
SYSTEM DESIGN STUDY

FINAL REPORT

Contract No. NAS 9-13467
Exhibit C

Prepared by

Gaylord K. Huth
Bruce D. Trumpis
Sergei Udalov

Axiomatix
13900 Panay Way, Suite 110M
Marina del Rey, California 90291

Prepared for

NASA Lyndon B. Johnson Space Center
Houston, Texas 77058

Axiomatix Report No. R7504-1
April 25, 1975

1

TABLE OF CONTENTS

LIST OF FIGURES

iii

1.0   INTRODUCTION

This report summarizes the results of several study tasks pertaining to various aspects of Space Shuttle communication system. The tasks performed can be logically divided into the following four categories:

1. Study of burst error correction for Shuttle command channels.

2. Performance optimization and design considerations for Costas receivers with and without bandpass limiting.

3. Investigation of experimental techniques for measuring low level spectral components of microwave signals, and

4. Investigation and comparison of potential modulation and coding techniques for the Ku-band return link.

Section 2 defines the motivation for the study tasks undertaken. A summary of burst error correction study is given in Section 3 with the details in References 1 and 2. Studies pertaining to optimization of Costas receivers are presented in Section 4 with the details in References 3 and 4. Investigation of the experimental techniques for spectrum measurement are summarized in Section 5 with details in Reference 5. Studies related to Ku-band modulation formats are discussed in Section 6 with details in References 6 and 7. Coding and decoding considerations for the 50 Mbps Ku-band link are also considered in Section 6.

l

2.0   MOTIVATION

Depending on the particular mission and the phase of the mission, the Space Shuttle will utilize either the S-band or the Ku-band communication links. The S-band communication can be carried out either directly between the Shuttle and the supporting ground stations such as the Space Tracking and Data Network (STDN) or via a tracking and data relay satellite system (TDRSS). The Ku-band link, however, will be established only via TDRS and will provide the Shuttle with a wideband[*] capability during the "on-orbit" phase of the mission.

Because of restrictions placed on the antenna dimensions and RF power limitations at both the Shuttle and the TDRS, the S-band link will have to operate at E_s/N_0 values of less than 0 dB. In fact, the threshold design point for the forward S-band link is at $E_s/N_0 = -5$ dB. This implies that particular attention must be paid to the design of this link to obtain maximum efficiency. Coding, burst error correction, and an optimized demodulator must be employed. These techniques, of course, are also applicable to the Ku-band link. Coding has been extensively analyzed and documented as a part of an earlier effort (References 8 and 9). Convolutional encoding and Viterbi decoding has been recommended and accepted as a technique for improving bit error probability of the weak links. This technique, however, while providing improved signal margins, has a side effect of generating error bursts which are particularly deleterious to the operation of the command portion of the S-band forward link. Consequently, the purpose of the studies summarized in Section 3 of this report was to develop a burst error correction scheme to protect the forward link commands against this type of error.

Because all of the S-band and most of the Ku-band digital channels utilize phase-shift keyed (PSK) suppressed carrier modulation, either a squaring or a Costas loop must be used by the receivers for carrier tracking and data recovery. Of the two loops, the Costas demodulator is generally

---

[*]Up to 1 Mbps on the forward links and up to 50 Mbps on the return links.

the easier one to implement, and hence this type of demodulator is commonly used in digital data receivers. Similar to the squaring loop, the Costas demodulator employs a nonlinear device--in this case a multiplier, which results in a "squaring" loss. This squaring loss becomes a major limiting factor when the E_s/N_0 ratio within the arm filter bandwidth of the Costas loop gets close to 0 dB or becomes negative, which is the case with a marginal link. The purpose of the arm filters is to prefilter the data signals prior to application to the multiplier which recovers the carrier tracking error from the data signals. Thus, it is evident that the efficiency of arm filtering plays an important role in determining the squaring loss generated by the multiplier.

Although a considerable amount of analytical work has been carried out and documented on the subject of Costas demodulator performance, the effect of arm filters on data distortion, which in turn determines the squaring loss has not previously been considered in detail. Thus, the task summarized in Section 4.1 is specifically directed towards defining the relationship between the arm filter bandwidth, the roll-off characteristics, the data rate, and the squaring loss. The specific case considered is that of Manchester data. As a result of this task, the arm filter characteristics which minimize squaring loss are established for a Costas loop. The results are particularly useful for optimizing threshold performance of the Costas demodulators used for the Shuttle's S-band and Ku-band links.

In addition to the optimization of the arm filters, a related study was carried out to determine the effect of a bandpass limiter on the performance of the Costas demodulator. Bandpass limiters, like automatic gain control (AGC), are commonly included ahead of the Costas demodulator to restrict the absolute level of signal-plus noise power applied to the demodulator and thus to maintain the design point parameters of the carrier tracking loop.

However, because the limiter is a nonlinear element, it affects the performance of the demodulator. Of specific significance is the performance degradation introduced by the limiter at low signal-to-noise ratios. As a result of this additional study task, quantitative data useful for Shuttle

link receiver optimization are derived. The results are summarized in Section 4.2.

The investigation of techniques for microwave signal spectrum measurement, as summarized in Section 5, was motivated by the requirements to maintain tight specifications on spurious radiations of the S-band link transmitters. Several experimental approaches are described, and the technique involving a commercially available test set is recommended.

Ku-band link modulation techniques are still under consideration. The most probable candidate for digital transmission is quadriphase multiplexing of two, and possibly three, digital channels. Interplex and similar techniques have been investigated and their capabilities and limitations have been defined. The techniques considered are summarized in Section 6.

3.0   SUMMARY OF BURST ERROR CORRECTION FOR THE
       SPACE SHUTTLE COMMAND CHANNELS

Up to now, the requirements on the command channel have been that the probability of command rejection, P_r, be less than 10^{-2} and the probability of false acceptance, P_{fa}, be less than 10^{-18}. These requirements were easily met with a (127,50) BCH command code and an error detector. A study was initiated to see if there was some method to decrease P_r with no increase in signal power. The detailed results of this study are given in Reference 1.

The uplinks or command links considered were from the STDN, SCF, and TDRS to the Orbiter. The last two of these links output error bursts into the command word so a burst error decoder was chosen over a random error decoder. A burst decoder was derived for cyclic codes; the implementation of such a decoder for the (127,50) command code is shown in Figures 1 and 2. Note that this decoder is only slightly more complex than the error detector.

The command rejection performance of the burst decoder and the error detector is shown in Figures 3, 4, and 5 for the three S-band links. The performance increase is at least two orders of magnitude. The probability of false acceptance performance is shown in Figure 6. Note that the 10^{-18} requirement can be met at reasonable bit error rates.

T_1 = "1" for cycle time 129-255
T_2 = "1" for cycle time 2-128
T_3 = "1" for cycle time 1
T_4 = "1" for cycle time 129-130
T_5 = "1" for cycle time 131-178

| 77 | 48 | D_2 | D_1 | D_3 |

128-bit Received
Command Word

127-bit Word Buffer
Received

D_3

| D_1 | D_2 |

48-bit Command Buffer
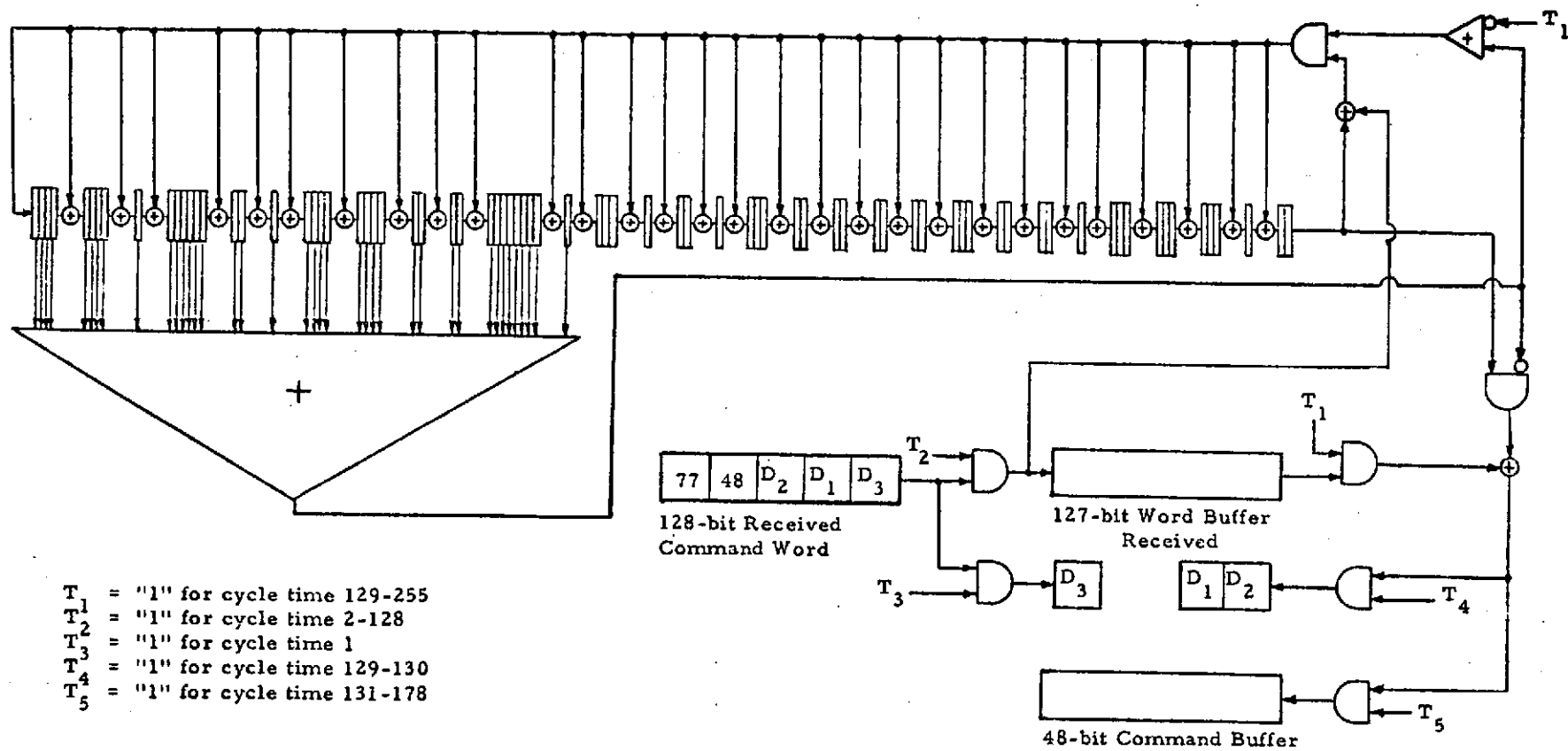
Figure 1.   A Burst Correcting Decoder (127, 50) BCH Code
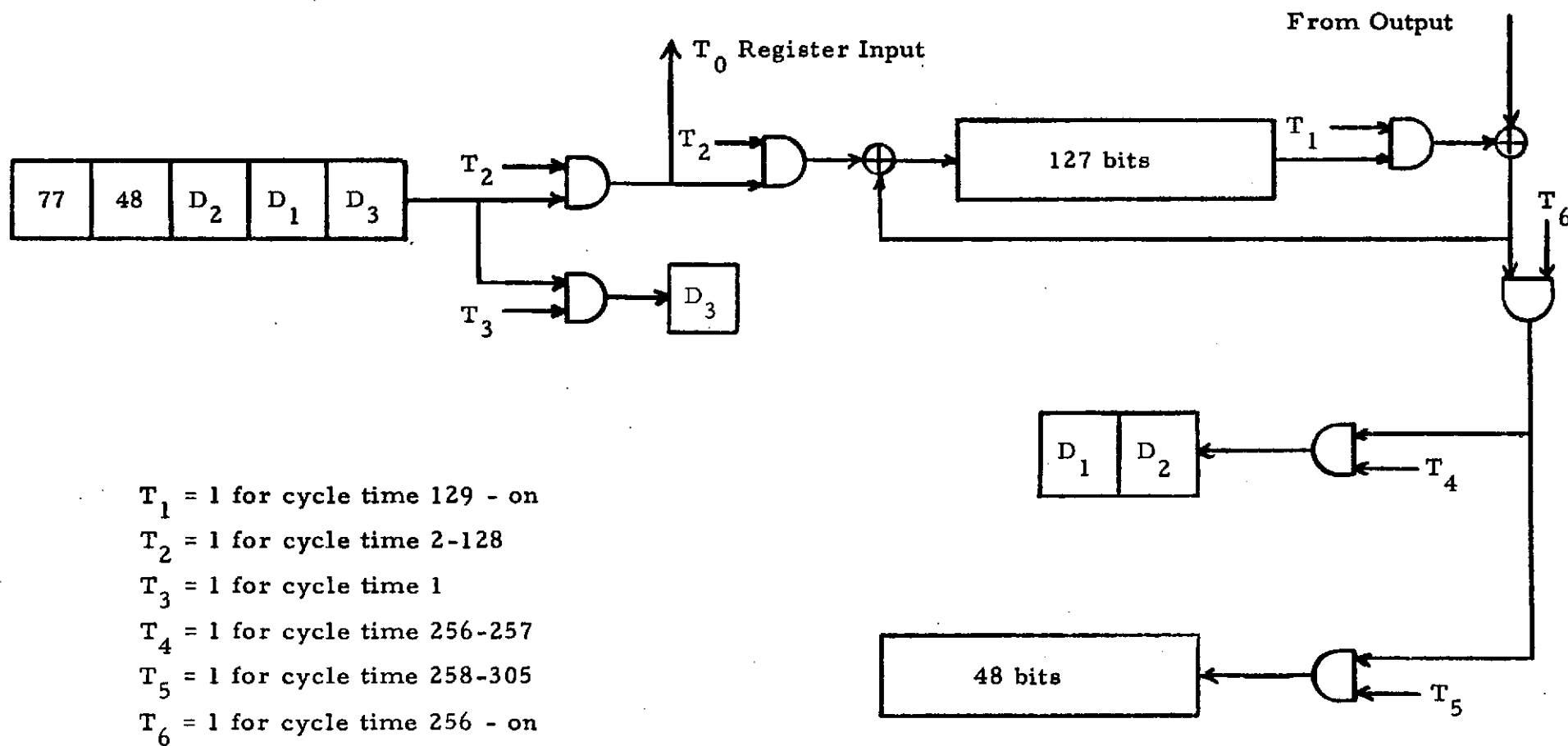
Figure 2. Revised Circuitry for Burst Decoder

Probability of Command Rejection, P_r

Probability of Bit Error, p

Burst Corrector

Error Detector

Figure 3

Command Channel Performance
for STDN-to-Orbiter and
Orbiter-to-NASA Payload Links

8

Probability of Command Rejection, P_r

Probability of Bit Error, p

Burst Corrector

Error Detector

Figure 4
Command Channel Performance
for SCF-to-Orbiter Link

9

Probability of Command Rejection, P_r

Probability of Bit Error, P_B

Burst Corrector

Error Detector

Command Channel Performance
for TDRSS-to-Orbiter Link

Figure 5

Figure 6. Probability of False Acceptance vs. Probability of Bit Error for Burst Decoder

4.0   COSTAS RECEIVER PERFORMANCE CONSIDERATIONS

4.1   Summary of "Optimum Performance of Costas Type Receivers"

This section addresses several problem areas associated with the design and optimum performance of suppressed carrier tracking receivers. In particular, the design of a Costas loop with both active and passive filters in the loop arms is considered for the case where the usual restrictive assumption that the arm filters are sufficiently wide to pass the data modulation undistorted is not imposed.[*] This leads to some new and important results concerning the optimum choice of arm filter bandwidths and spectral roll-off. Use of the results in a design lead to the most noise immune loop that can be constructed using passive arm filters.

Since the MAP estimator for the signal phase is a Costas-type loop with integrate and dump circuits in the arms when symbol sync is known, the noise immunity of the approach is derived and compared with that of a Costas loop containing a variety of passive arm filters. In fact, in the region of symbol energy-to-noise ratio R_d of 0 to -10 dB, it is shown (see Figure 7) that the use of symbol sync to operate the integrate-and-dump arm filters gives approximately 5 dB of improvement in required carrier power-to-noise ratio C/N_0 over passive RC-type arm filters. For 4-pole Butterworth filters, the improvement is of the order of 4 dB. This comparison is extended to the case of ideal (rectangular) arm filters. Here the improvement is only 2.5 dB. The improvement demonstrated is not only realized during tracking but can also be made effective during sync acquisition. This is felt to be of considerable importance in the design and operation philosophy of the TDRS links.

The effect of arm filter distortion is studied in detail. The analysis shows that there is an optimum bandwidth for each type of filter that is a function of R_d. These results are depicted in Figure 8.

The Costas loop configuration with integrate-and-dump arm filters requires accurate estimates of symbol timing; however, symbol sync normally requires carrier demodulation. It is shown, under ideal conditions,

[*]Manchester coded data is assumed.

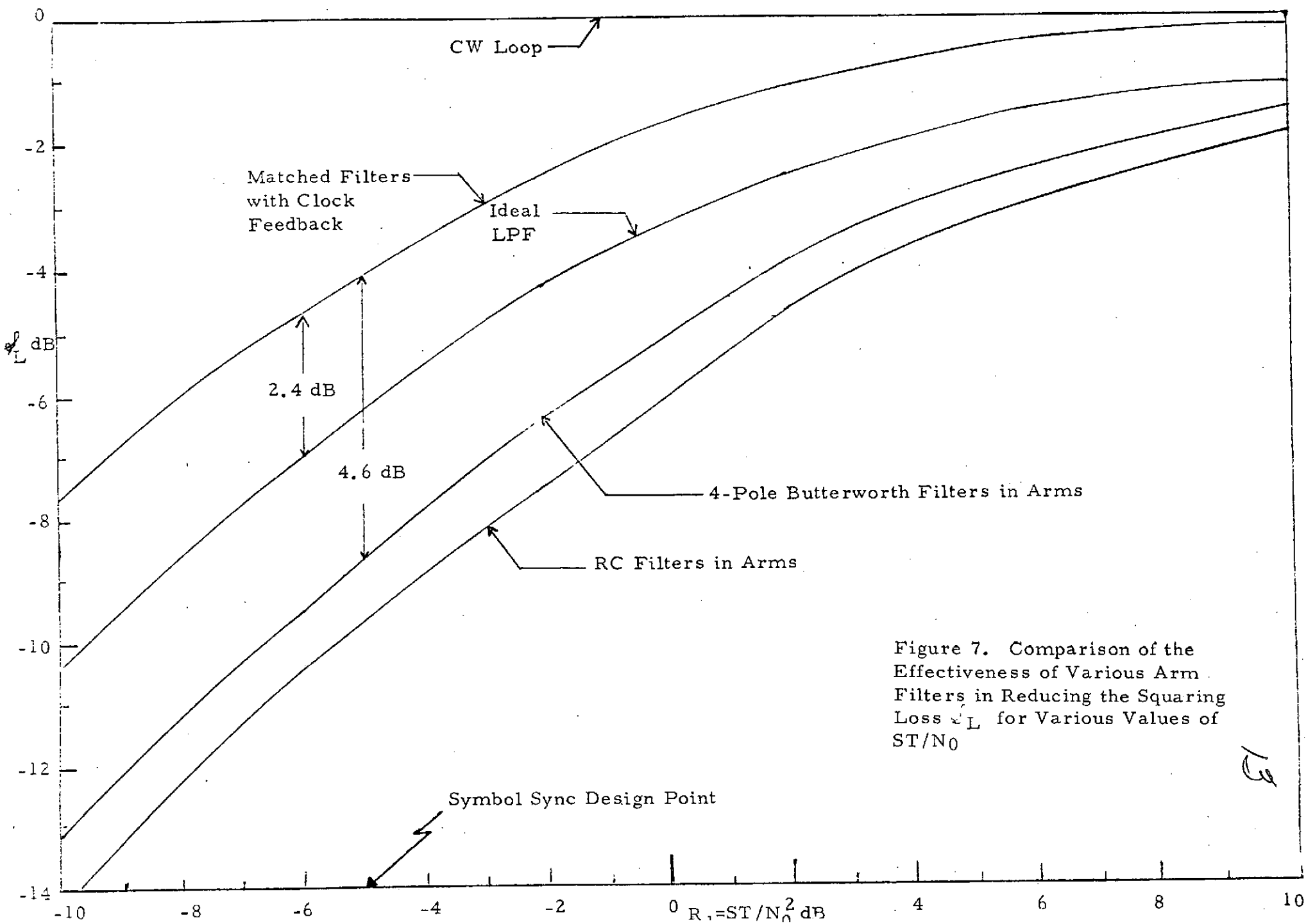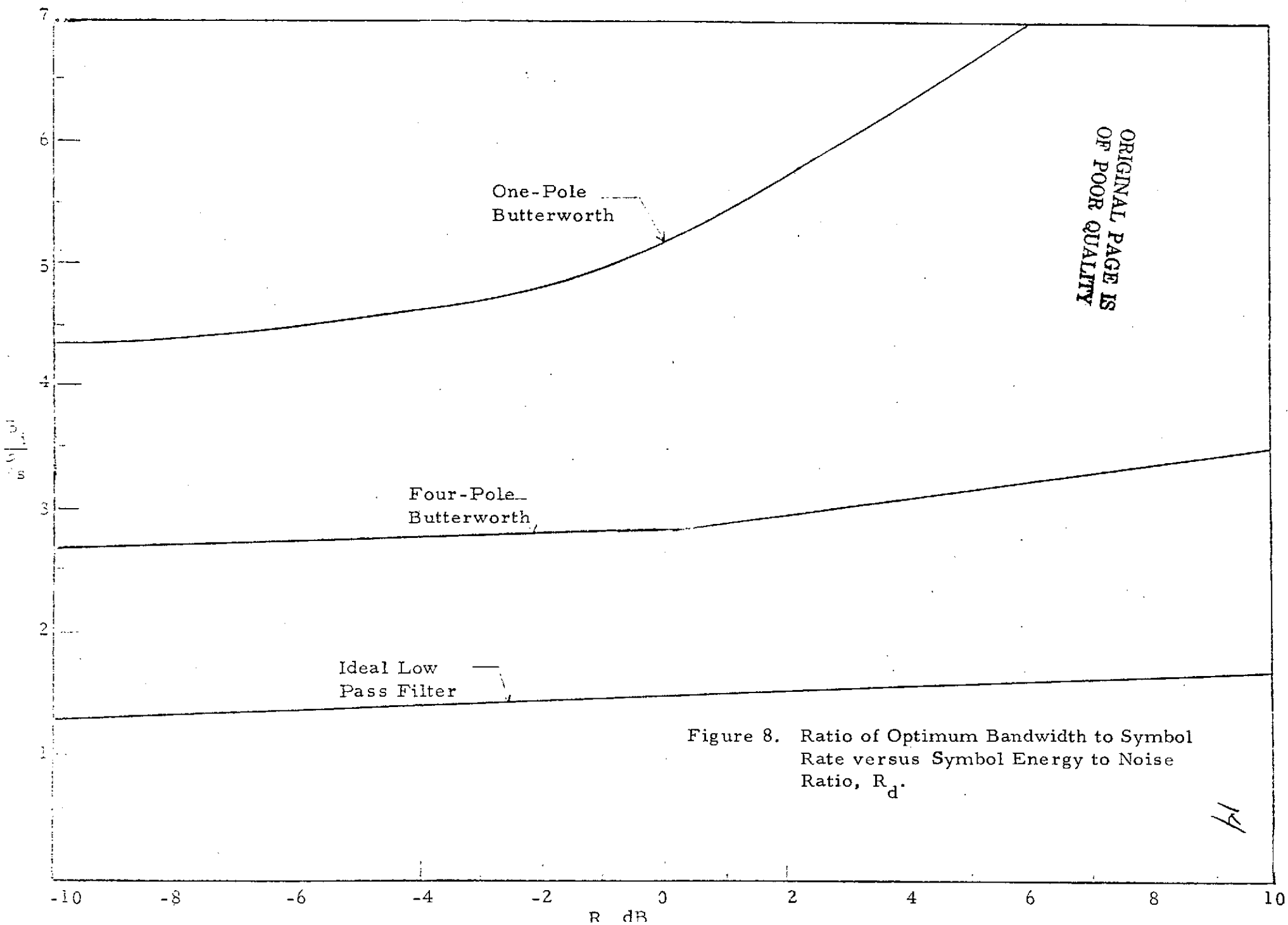Figure 7. Comparison of the Effectiveness of Various Arm Filters in Reducing the Squaring Loss $\mathcal{L}_L$ for Various Values of ST/N_0

Figure 8. Ratio of Optimum Bandwidth to Symbol Rate versus Symbol Energy to Noise Ratio, R_d.

One-Pole Butterworth

Four-Pole Butterworth

Ideal Low Pass Filter

that symbol sync can occur prior to carrier acquisition. But further work is needed since neither the effect of inaccurate clock timing nor IF filtering which can produce intersymbol interference is considered.

4.2   Summary of Design and Performance of Costas Receivers Containing Bandpass Limiters

This section addresses several key questions and gives various new results in the design of a Costas tracking loop preceded by a bandpass limiter (BPL). The BPL is required to control the signal amplitude at the loop input during carrier acquisition when the coherent AGC is not operating properly.

As in the previous section, the squaring loss of the combined BPL/ Costas loop was derived assuming a hard limiter, and optimum arm filter bandwidths were found.[*] This result is shown in Figure 9, and we note that these bandwidths differ from those computed for a Costas loop without a BPL. The minimized squaring loss for the BPL/Costas loop is considerably more than for the Costas loop alone. The addition loss due to the BPL is shown in Figure 10.

A new expression for the signal amplitude suppression factor due to a BPL preceding a Costas loop was derived and compared to that for a phase locked loop, as shown in Figure 11. Figure 12 shows the variation in loop bandwidth with signal level due to the signal suppression phenomenon.

---

[*]Manchester encoded data is assumed.

Figure 9. Ratio $B_i/\mathcal{R}_s$ Which Minimizes the Squaring Loss Versus R_d.
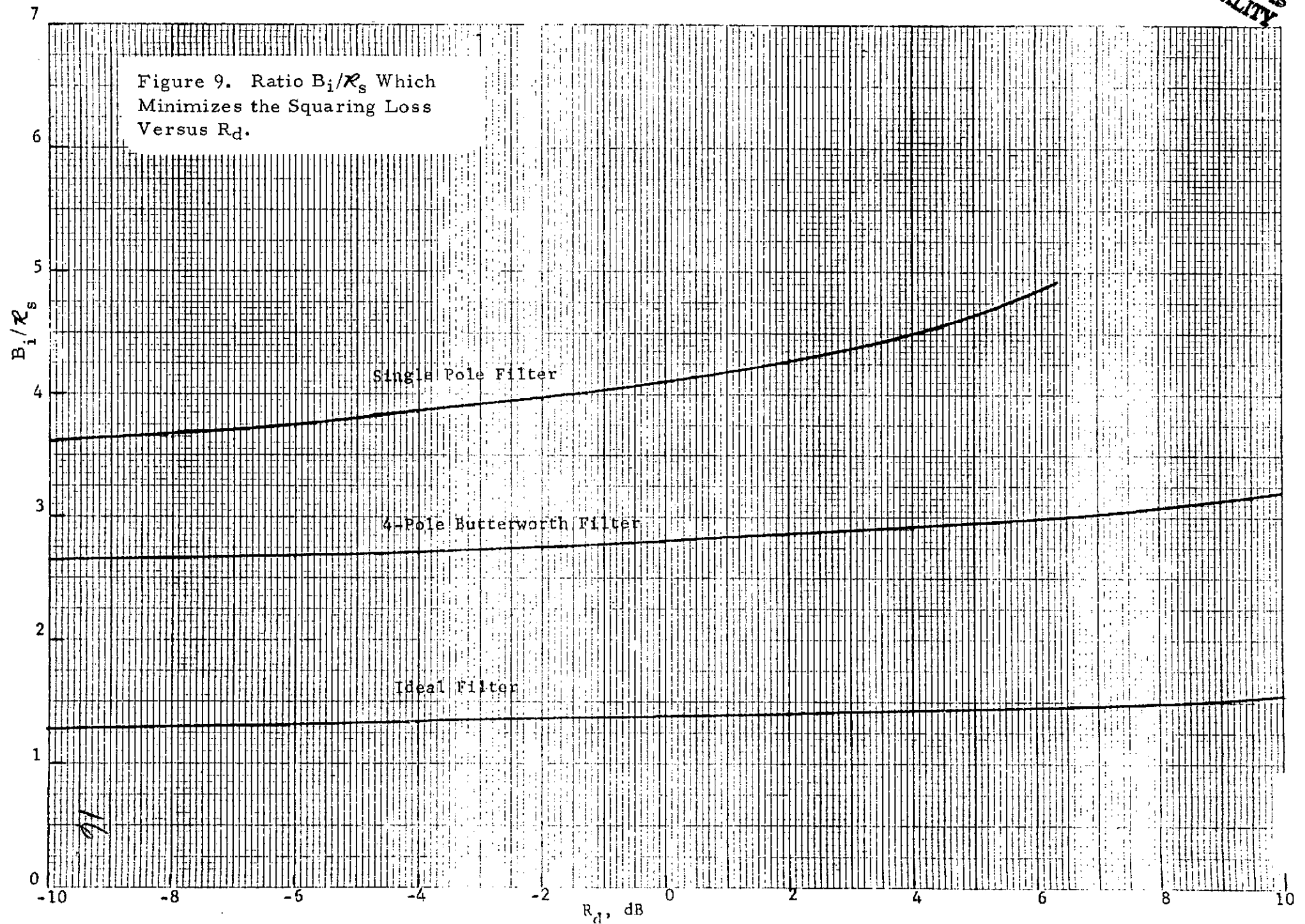
Figure 10. Loss in Loop Signal-to-Noise Ratio Due to the Presence of a Limiter for Various Values of R_d.

Ideal Filter

4-Pole Butterworth Filter

Single Pole Filter

Shuttle Design Point

NOTE: The optimum value of $B_i/\mathcal{R}_s$ is used here.

L, dB

R, dB

Figure 11. Signal Amplitude Suppression Factor Versus IF SNR for the CW and Costas Loop.

Signal Suppression

$\widetilde{\alpha}_1$

$\widetilde{\alpha}_s^2$

Ideal Filter
4-Pole Butterworth Filter
Single-Pole Filter

ρ_H, dB

-20 -18 -16 -14 -12 -10 -8 -6 -4 -2 0

18
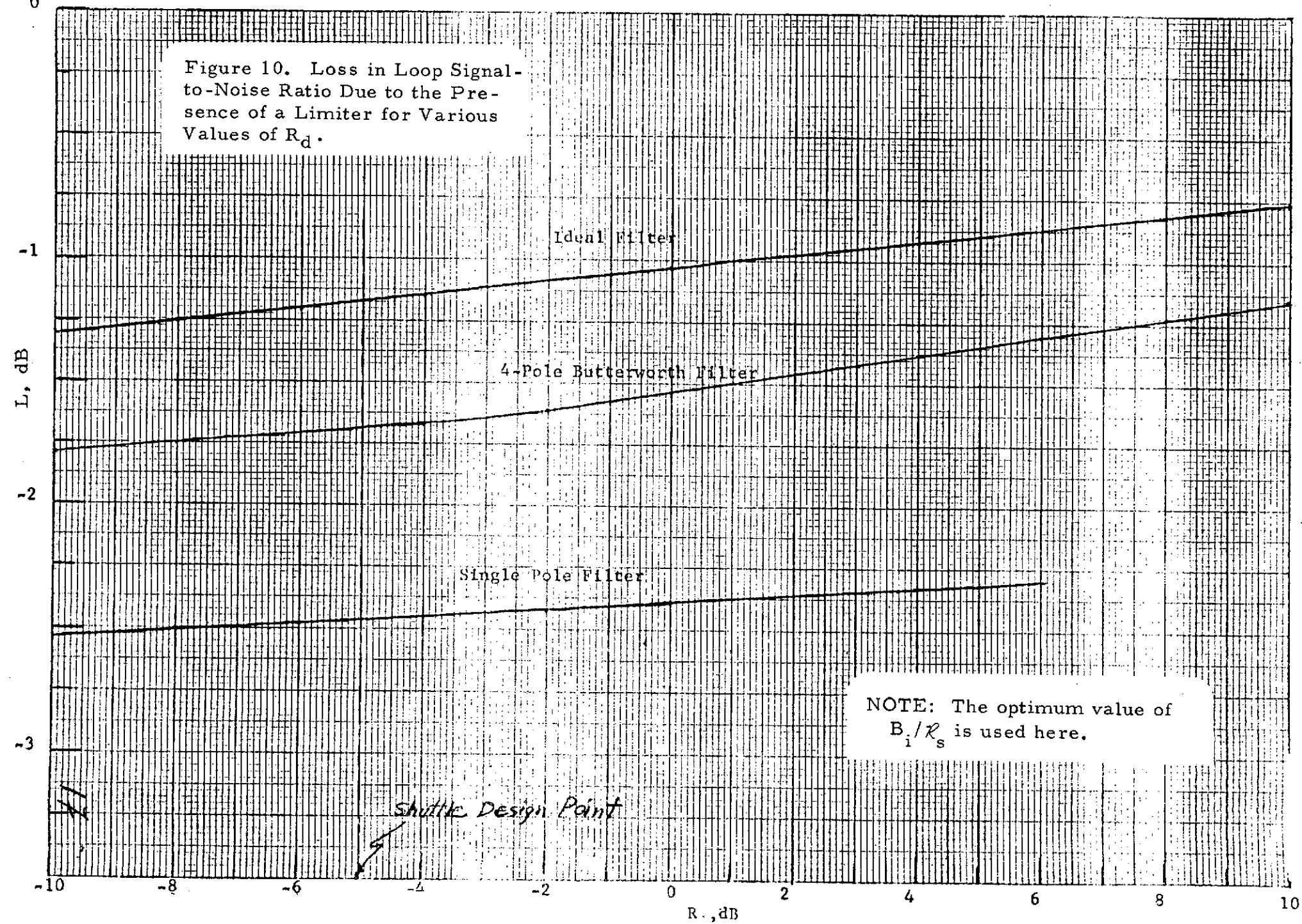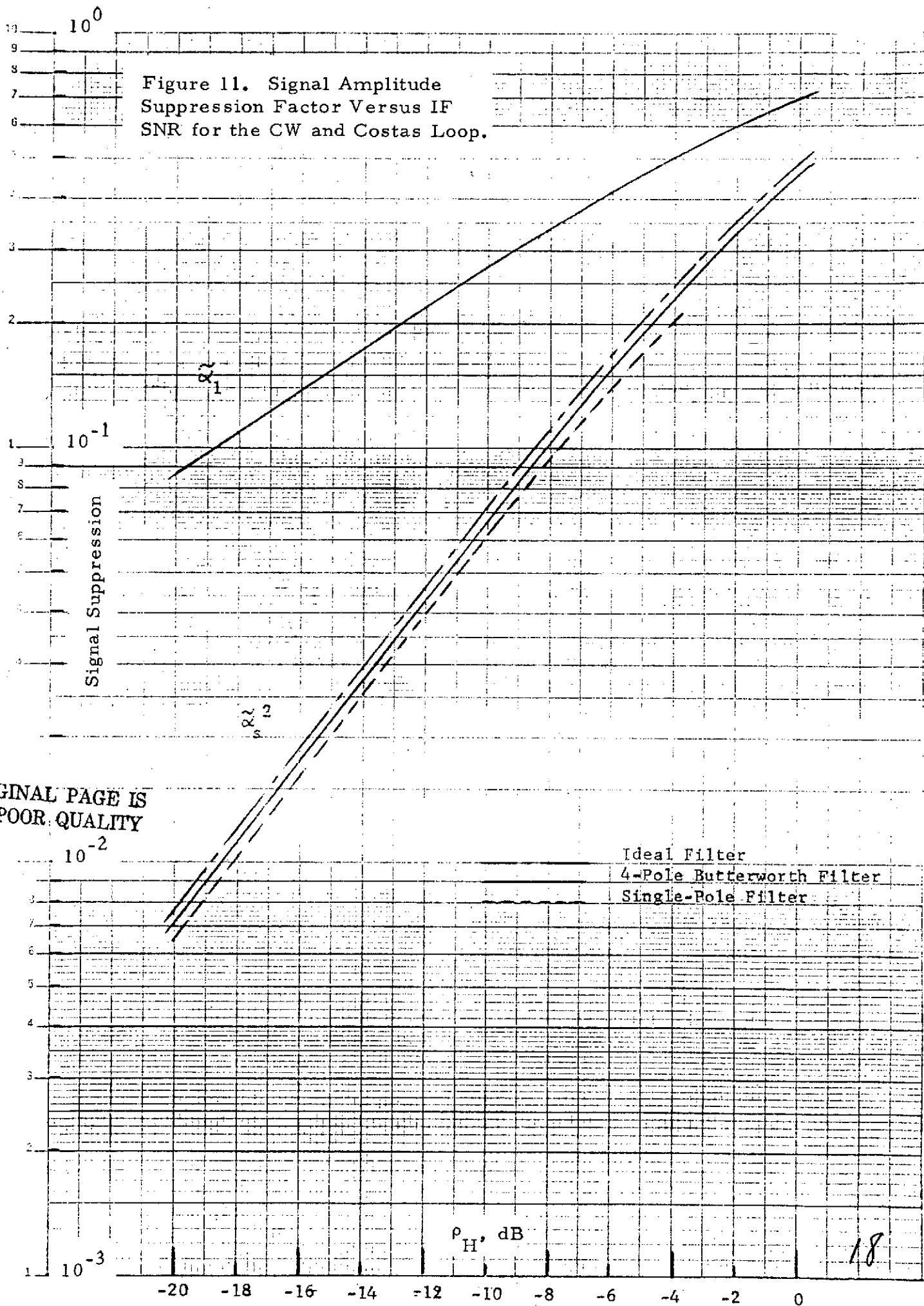
Figure 12. Variation of Loop Bandwidth with Signal Level for Optimum Values of $B_i/\mathcal{R}_s$

B_L/B_{L0}

RC Filter, 4-Pole Butterworth or Ideal Filter

10^2

10^3

10^1

10^0

R_d, dB

R_d, dB

-8   -6   -4   -2   0   2   4   6

19
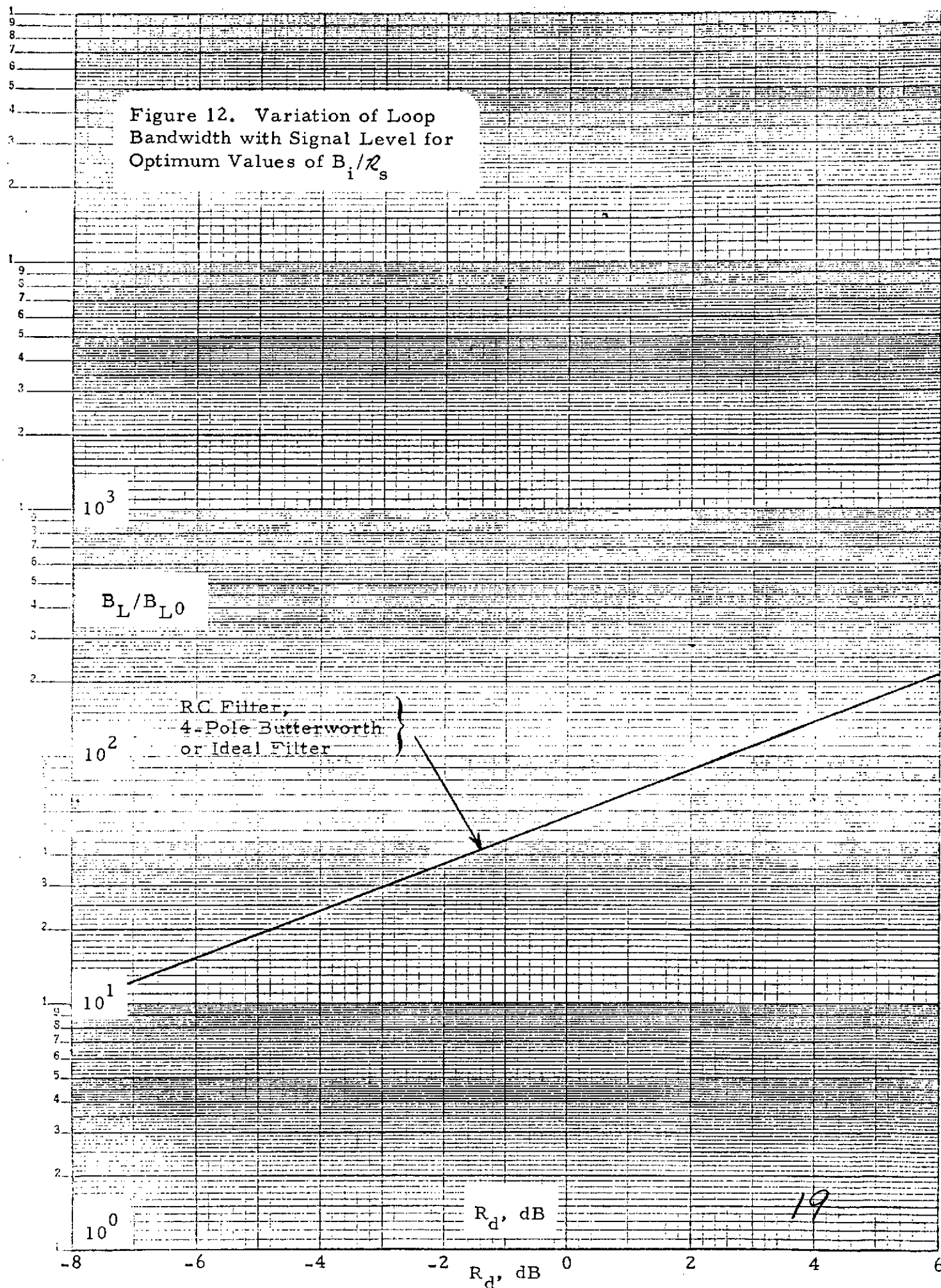
5.0   SUMMARY OF EXPERIMENTAL TECHNIQUES FOR MEASURING
       LOW LEVEL SPECTRAL COMPONENTS OF MICROWAVE SIGNALS

The requirements placed on spectral purity of Space Shuttle micro-
wave communication transmitters demand control of spurious radiations.
In addition to the noise floor resulting from the multiplication of crystal
oscillator output frequencies to microwave region, various interfaces
between equipment subunits may result in discrete spectral components.
Although very small, these components may exceed the specification placed
on the systems performance.

The dynamic range and frequency resolution limitations of conven-
tional frequency-swept spectrum analyzers generally preclude the use of
these instruments from detecting extremely low level spectral components
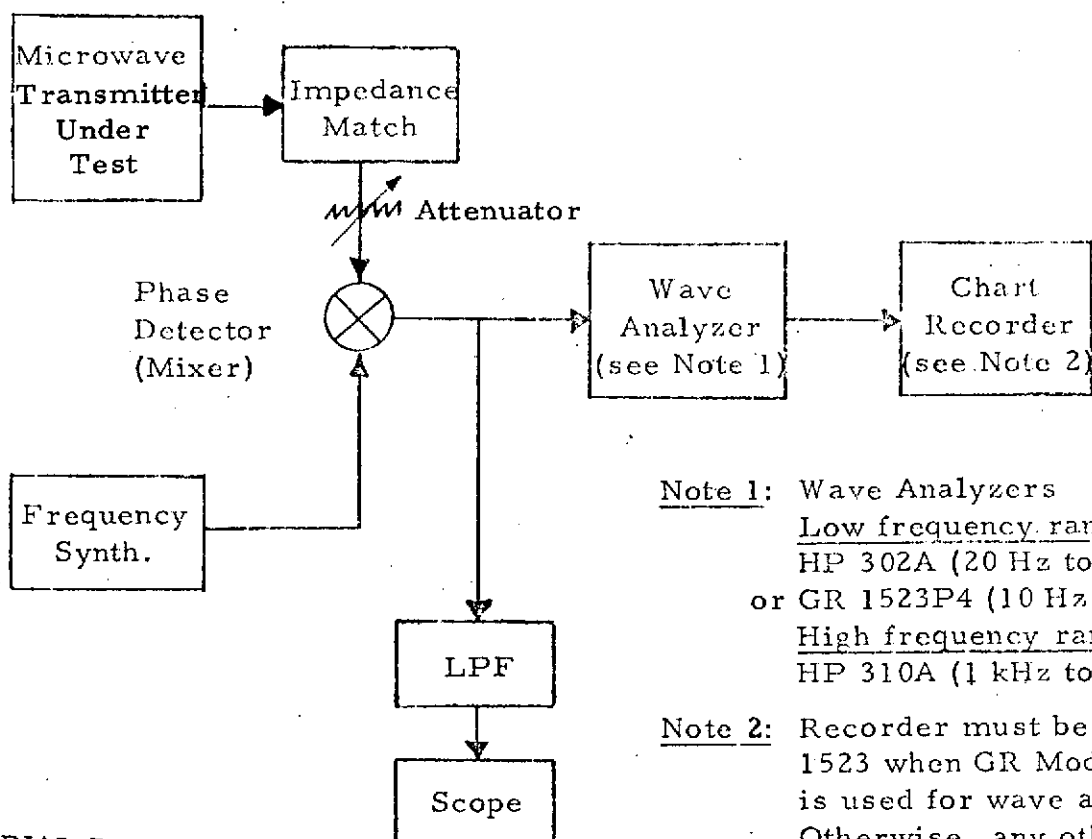of the microwave transmitters. Consequently, specialized techniques for
measuring spectral purity of the microwave transmitter must be devised
to test the compliance of any particular system with its specifications.

One of these specialized techniques involves the translation of the
microwave RF spectrum to baseband. The translation is accomplished by
mixing the RF microwave signal with a clean CW signal whose frequency
is either exactly equal to or is offset by a certain amount from the carrier
frequency of the measured signal. The resulting baseband spectrum is then
investigated by a low frequency wave analyzer whose output, in turn, can be
displayed on a chart recorder. A typical test setup and a corresponding
hypothetical spectrum are shown in part (a) and part (b) of Figure 13,
respectively.

The limitation of this technique is that it requires a very stable
reference oscillator and a phase detector (mixer) which is linear over the
dynamic range of signal fluctuation expected from the test signal.

An alternate technique employs a phase-locked loop (PLL) for the
translation of the RF signal sidebands to the baseband. Because the loop's
voltage-controlled oscillator (VCO) automatically locks to the transmitter's
carrier frequency and average phase, the problem of matching the test and

Microwave Transmitter Under Test

Impedance Match

Attenuator

Phase Detector (Mixer)

Wave Analyzer (see Note 1)

Chart Recorder (see Note 2)

Frequency Synth.

Note 1: Wave Analyzers
Low frequency range:
HP 302A (20 Hz to 50 kHz)
or GR 1523P4 (10 Hz to 80 kHz)
High frequency range:
HP 310A (1 kHz to 1.5 MHz)

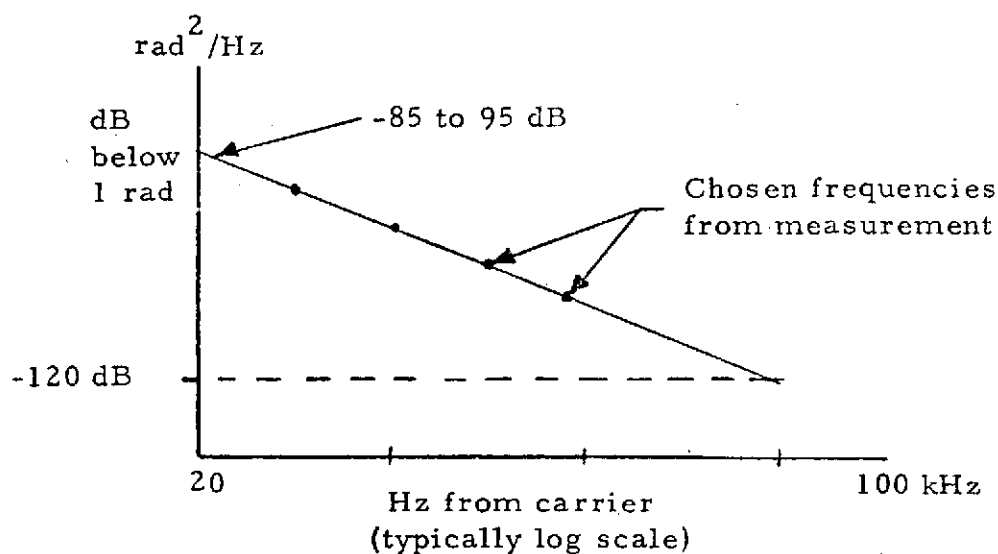Note 2: Recorder must be GR Model 1523 when GR Model 1523P4 is used for wave analysis. Otherwise, any other chart recorder having sufficient resolution can be used.

LPF

Scope

(a) Typical Test Setup

rad^2/Hz

dB below 1 rad

-85 to 95 dB

Chosen frequencies from measurement

-120 dB

20

Hz from carrier
(typically log scale)

100 kHz

(b) Typical wave analyzer output

Figure 13. Low-Level Sideband Measurement

reference frequencies is eliminated. Furthermore, phase and frequency fluctuations whose rates fall within the bandwidth of the PLL are tracked out. This takes care of long- and medium-term frequency drifts.

On the other hand, phase noise and spurious frequency components which are outside the tracking loop bandwidth appear at the output of the phase detector of the PLL and can be applied to the input of the baseband spectrum analyzer. Assuming that amplitude instabilities of the transmitter's output and of the test equipment are extremely small, the phase detector output will contain only the components due to frequency or phase jitter, or both.

Test equipment which works on this principle is commercially available. A typical unit is FEL* Model 800B. The simplified block diagram for this device is shown in Figure 14. According to the manufacturer's specifications, the S-band phase noise floor of the 800B is below -100 dB (in 1 Hz bandwidth) at frequencies above 1 kHz away from the carrier. The low residual noise of the FEL phase jitter analyzer makes this equipment the logical choice for the detection of spurious components in the output spectra of the Shuttle's microwave transmitters.

---

*Frequency Engineering Laboratories, Farmingdale, New Jersey.
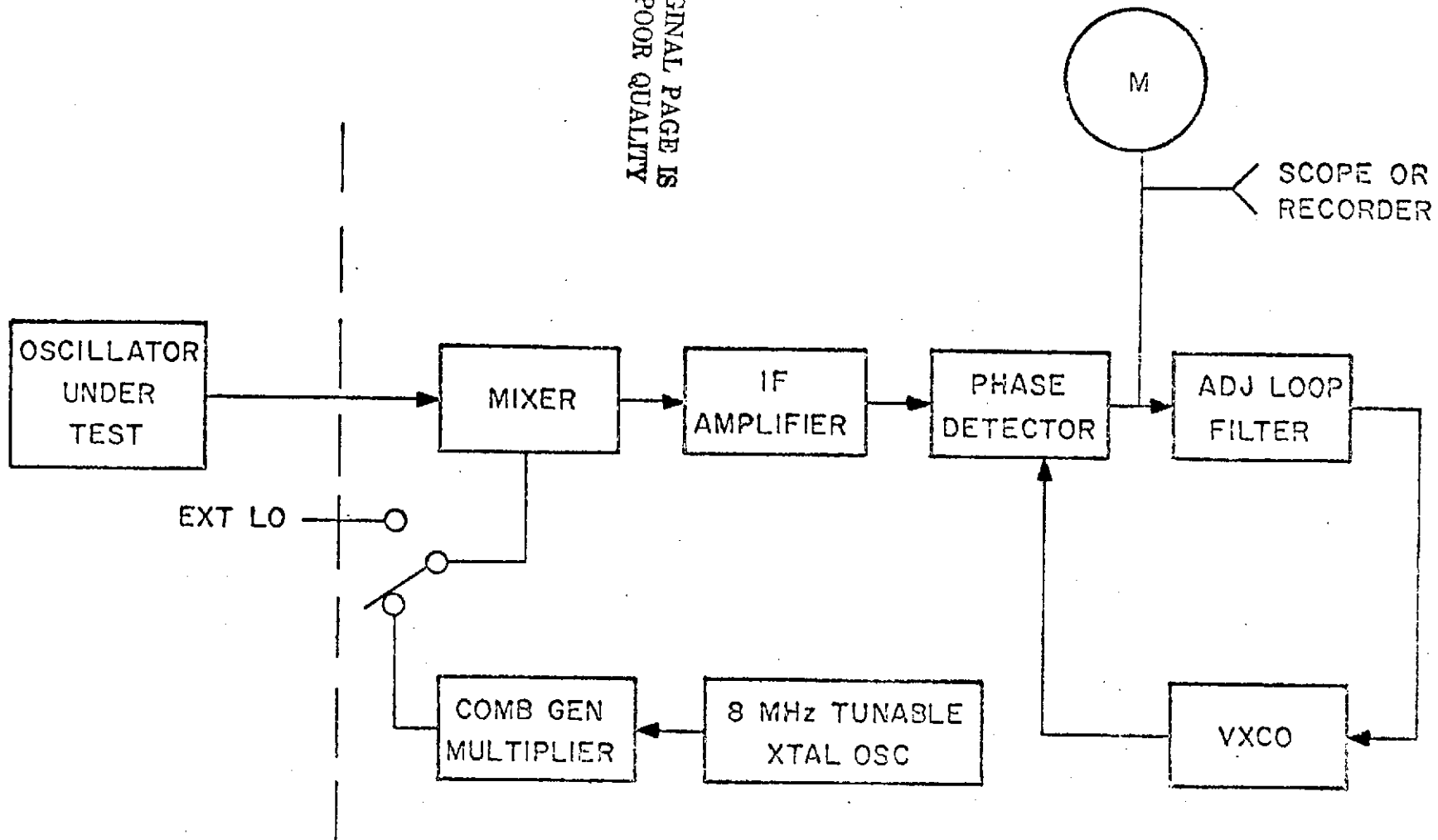
FIGURE 14.   800B SYSTEM BLOCK DIAGRAM

6.0   KU-BAND RETURN LINK MODULATION TECHNIQUES

6.1   Summary of Feasibility Study of an Interplex Modulation System for the Orbiter's Ku-Band Link

The requirement for the Orbiter's Ku-band return link calls for simultaneous transmission of at least two independent data channels, one having a rate of up to 50 Mbps and the other having a rate of up to 2 Mbps. It is also desirable, if feasible, to transmit a third data stream of operational data at a 192 kbps rate, in addition to the aforementioned data streams. Because these three channels have different clocks, they cannot be transmitted by time division multiplexing without employing a complex reclocking scheme. Consequently, other modulation techniques involving phase multiplexing and use of subcarriers must be considered. Interplex is one of such potentially applicable techniques.

The advantages of Interplex modulation as compared with conventional phase shift multiplexing is that it minimizes the amount of RF power wasted as intermodulation products and it also provides, under certain conditions, for complete suppression of the carrier component, thus allowing more power to be placed in the information-bearing sidebands. In this report, the analysis of a three-channel Interplex system was carried out to determine whether three data channels can be transmitted simultaneously. The modulator and demodulator for such implementation are shown in Figures 15 and 16, respectively. As shown in Figure 15, two lower rate data streams are bi-phase modulated on two separate subcarriers and the modulated subcarriers are then modulo-2 added with the high rate data stream. The composite signals are then summed and applied to a phase modulator.

For maximum suppression of the carrier and intermodulation components, the high rate data stream modulation is assigned the modulation index of ± 90 degrees, i.e., antipodal modulation. The phase modulation angles for the remaining channels are then assigned according to the relationship $\theta_n = \tan^{-1} \sqrt{a_n}$, where $a_n = P_n/P_1$ is the ratio of the power in
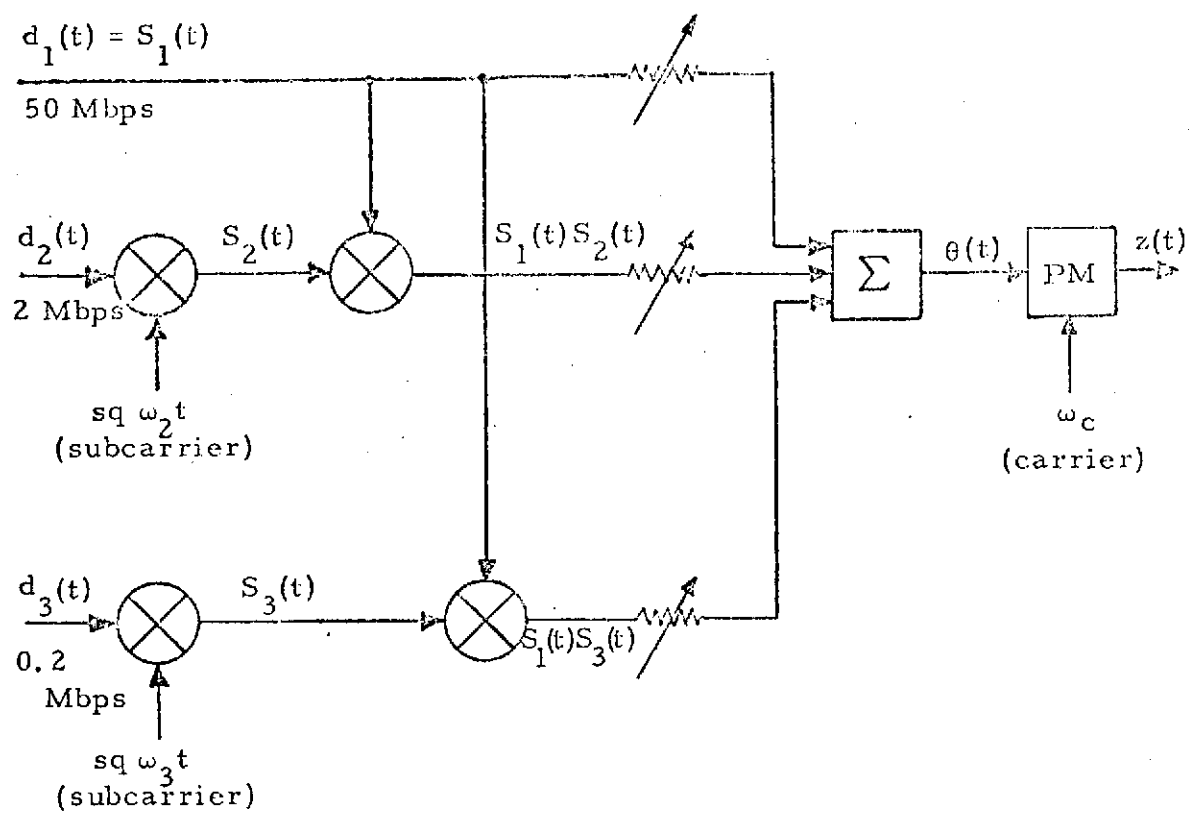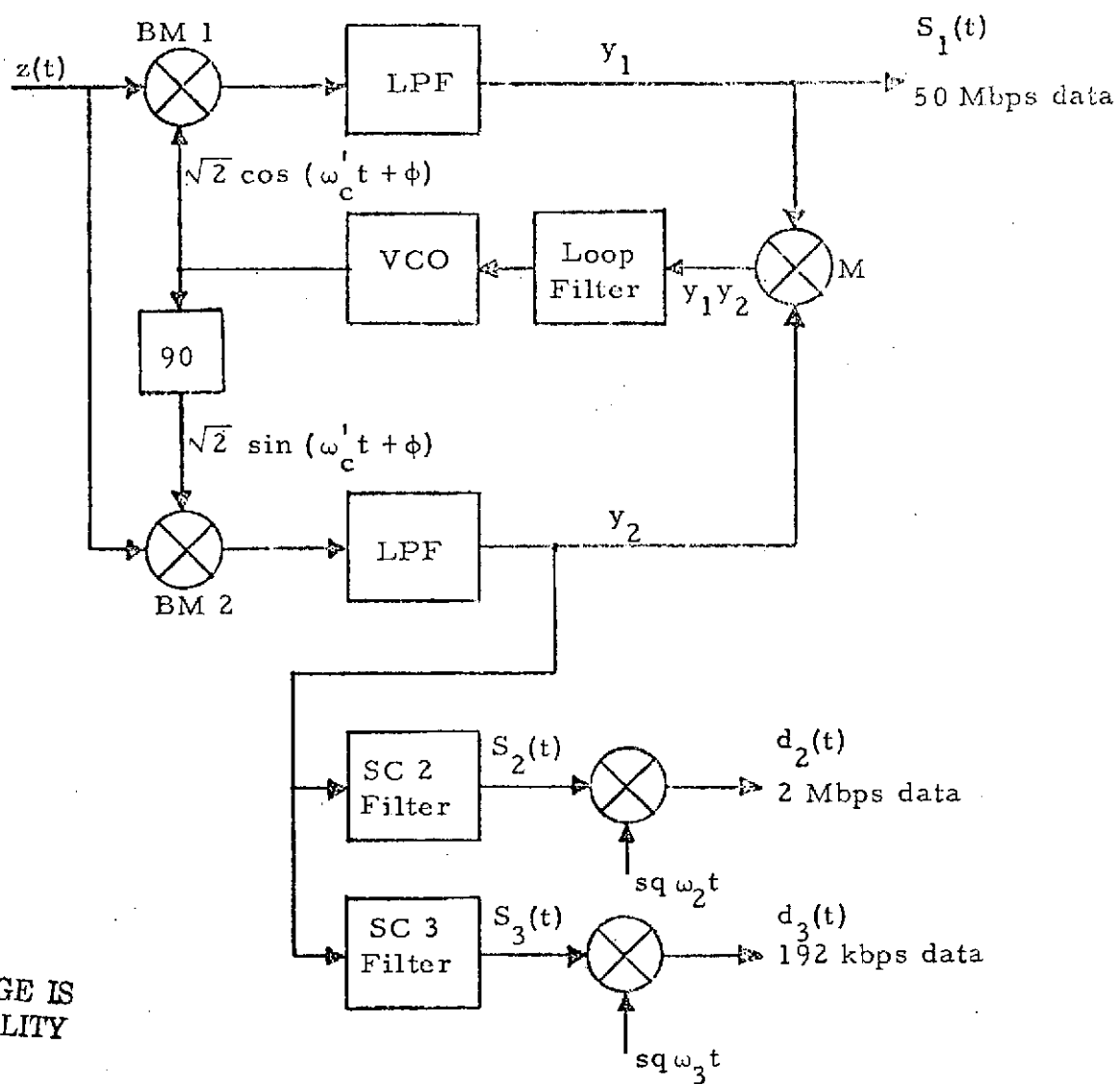
Figure 15. Three-Channel Interplex Modulator

Figure 16. Three-Channel Interplex Demodulator Block Diagram

the nth channel (n = 2, 3, ...) to the power in the "main" channel. In the report, we have used the equal error rate criterion for all three channels and thus the power allotted to the secondary channels was made proportional to the data rates.

Because most of the signal power is assigned to the antipodal (bi-phase) modulation, a Costas loop demodulator shown in Figure 16 can be used for carrier tracking and data recovery. The secondary data channel subcarriers are extracted from the lower (quadrature) arm of the Costas loop and, after filtering, the data is recovered by re-inserting the appropriate subcarriers. Although some penalty is paid for not using the energy in the secondary channels for carrier tracking, this penalty is generally small, typically less than 1 dB if the combined power in the secondary channels is at least 6 dB below the power in the primary channel.

When considering a multi-channel Interplex system, the crosstalk between the channels must be taken into account. Of primary concern in the crosstalk which is caused by the carrier tracking error. When this error is present in the demodulator loop, the primary channel data starts to appear in the secondary channels, and vice versa. However, for the secondary channel power assignments proportional to data rate, the crosstalk of the major channel into the secondary channel (worst case crosstalk) is 10 dB below the secondary channel signal if the carrier tracking error is less than 15 degrees in the numerical example presented in Reference 6. With a properly designed loop, carrier tracking error can be maintained below this value even for the worst case of Shuttle acceleration with respect to TDRS.

Thus, the conclusion of the study is that, at least in principle, a three-channel Interplex modulation/demodulation scheme can be mechanized to accommodate the requirements of the return Ku-band link.

6.2   Summary of Multiplexing Modulation Formats for the
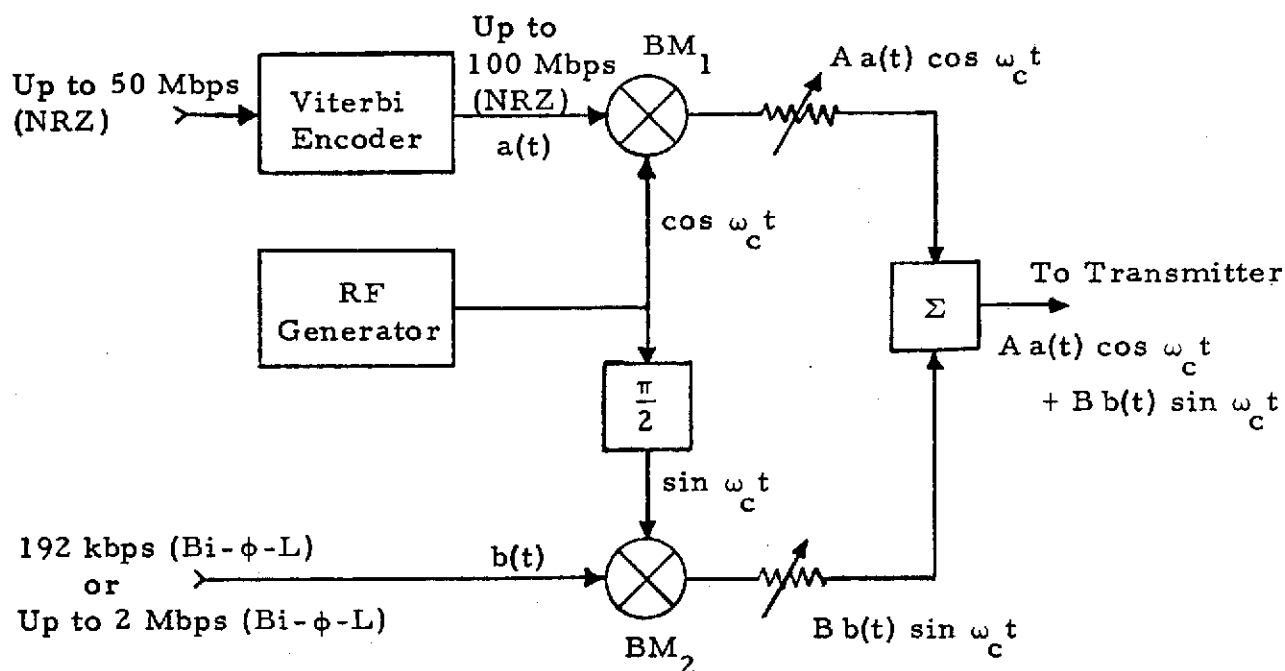   Orbiter's Ku-Band Return Link

Reference 7 considered various aspects of modulation format selection for the Ku-band return link. Specifically, the methods for modulation

and demodulation of return link data streams were considered. First, the relatively straightforward problem of transmitting only two data streams was considered. One possibility for achieving this is to use two orthogonal components of a single carrier, with each component being bi-phase modulated by its own data stream. The amplitudes of the two carrier components are then adjusted for the required power division and combined to yield a quadriphase modulated carrier. The rates of the two data streams can be different and their clocks do not have to be synchronous.

If the power in one of the orthogonal components exceeds the power in the second component by a significant amount, say by 6 dB or more, the simplest way to recover the data and to provide carrier tracking is to use a Costas loop demodulator. The demodulator then locks on to and tracks the strongest of the two orthogonal carrier components. The basic modulator/demodulator configurations for this scheme are shown in Figure 17.

With perfect carrier frequency and phase tracking, there is no cross-talk between the two recovered data streams because of the orthogonality of the two carriers. But if a carrier phase tracking error is present, cross-coupling develops between the two demodulated data streams. In addition to being a function of carrier tracking error, the crosscoupling is also a function of power division between the channels and their respective band-widths. In our study, we have considered the case where either the 192 kbps or the 2 Mbps data channel is quadriphase multiplexed with the 50 Mbps channel, the power in the 50 Mbps channel being four times the power of either the 192 kbps or the 2 Mbps data channels. Figure 18 shows the calculated data-to-crosstalk ratios vs. carrier tracking error for the afore-mentioned conditions. In the figure, the curves labeled $D_2(1)$ represent the ratio of either the 192 kbps or the 2 Mbps data to the crosstalk caused by by the 50 Mbps stream.* Conversely, the curve labeled $D_1(2)$ indicates data-to-crosstalk ratio in the 50 Mbps channel, the crosstalk being caused

---

*Because of 1/2 rate encoding, the symbol rate of this stream is 100 Mbps.

(a) Two-Channel Quadriphase Modulator
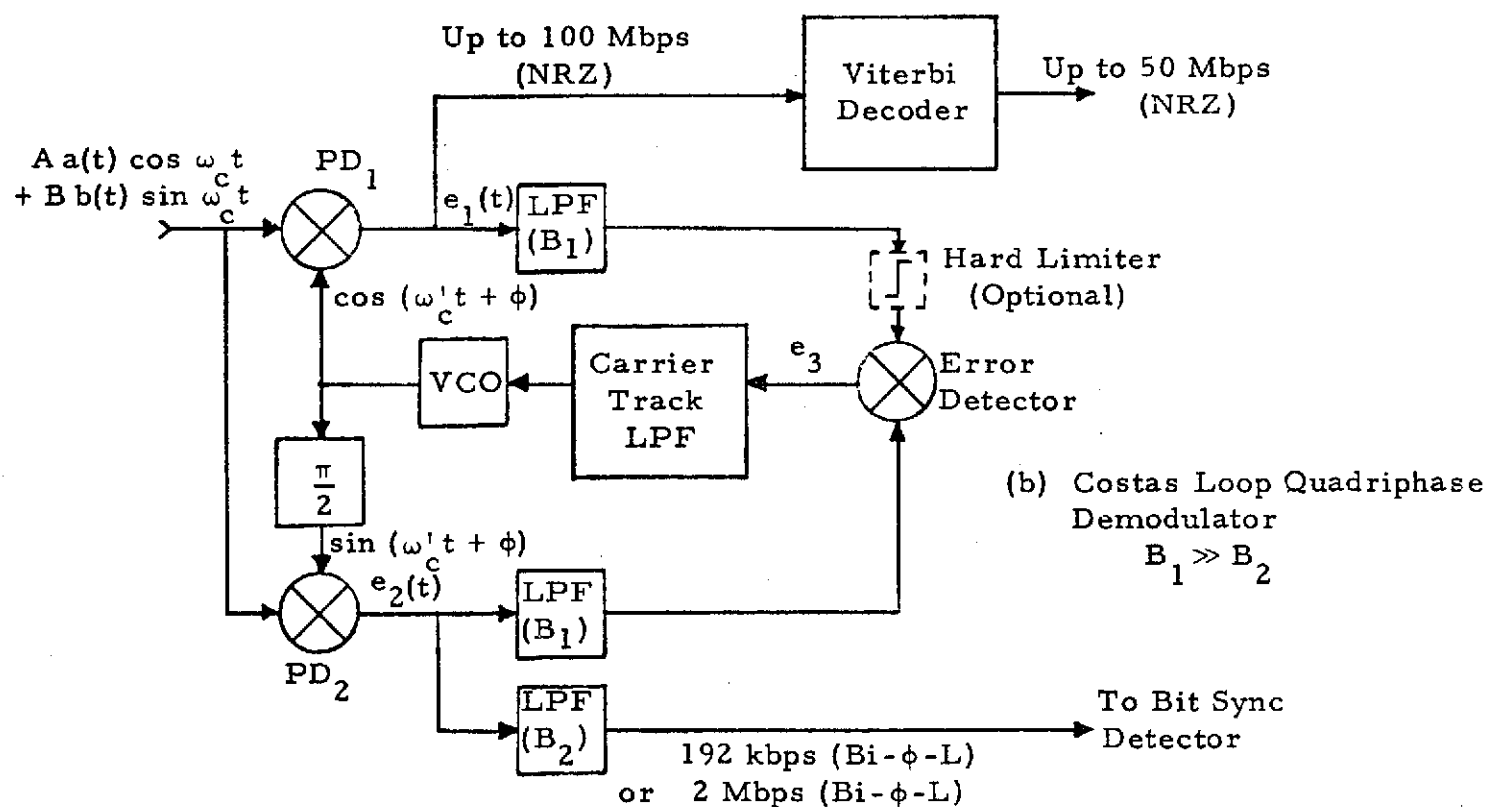
(b) Costas Loop Quadriphase Demodulator

$B_1 \gg B_2$

Figure 17. Basic Modulator/Demodulator Configuration for Ku-Band Return Link -- Mode 1

ORIGINAL PAGE IS
OF POOR QUALITY

$D_2(1)$
for 192 kbps

$D_2(1)$
for 2 Mbps

$D_1(2)$

Carrier Tracking Error ϕ (degrees)
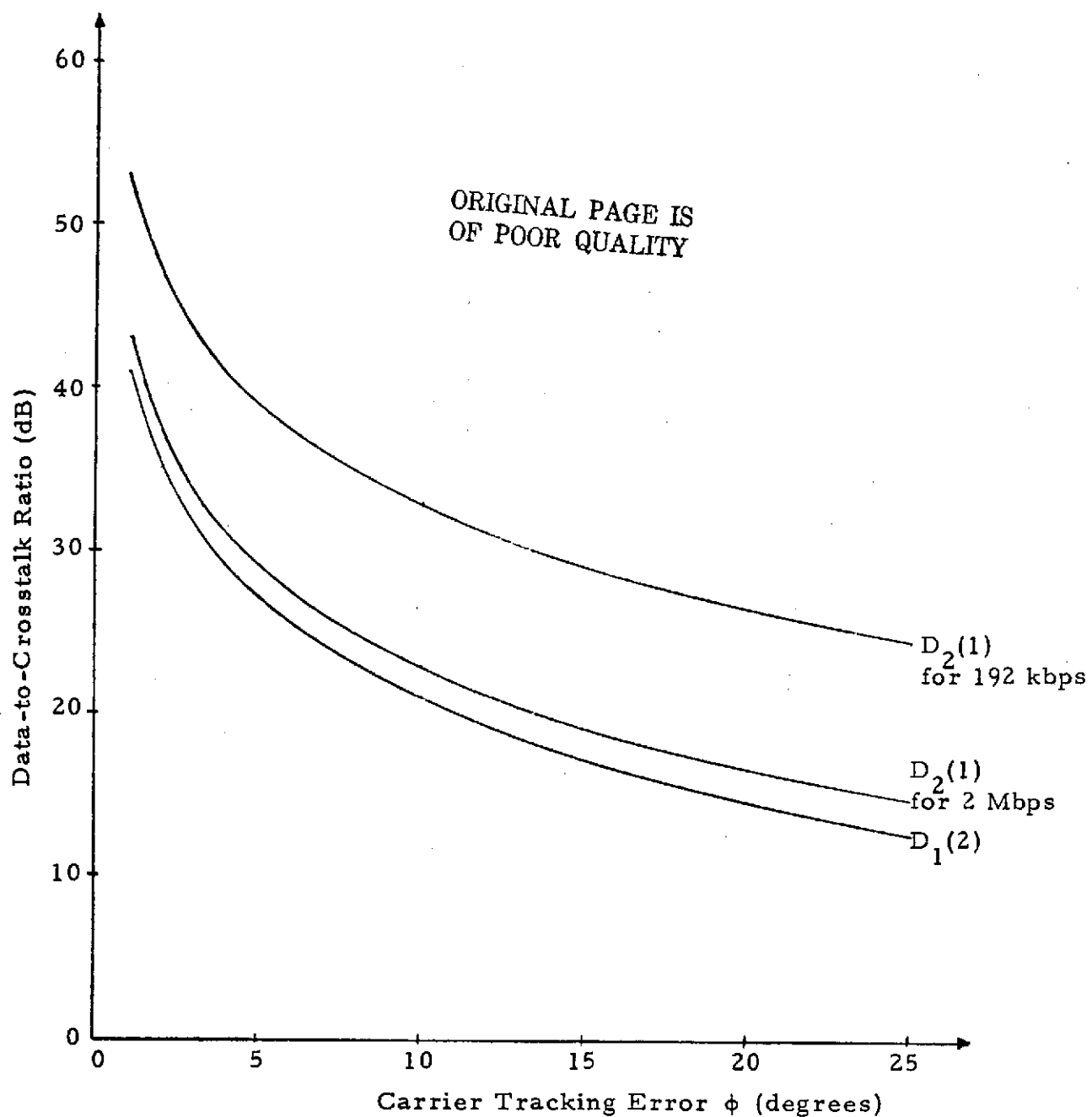
Data-to-Crosstalk Ratio (dB)

Figure 18. Data-to-Crosstalk Ratio vs. Carrier Tracking Error ϕ
for a Two-Channel Quadriphase Demodulator and
Power Ratio $P_1 = 4P_2$

by either one of the lower rate channels. We note, however, that for the case considered, the carrier phase error has to be over 25 degrees in order to reduce the worst case data-to-crosstalk ratio to about 10 dB, a ratio which is of the same order of magnitude as the E_b/N_0 for the 10^{-6} error rate. The 25 degree carrier error is, however, a relatively large error and with proper loop design can be minimized for the Orbiter-to-TDRS dynamics.

The crosstalk for a two-channel Interplex with the same power division, i.e., 4 to 1 power division, was also computed. It was shown that from the standpoint of crosstalk the quadriphase modulation and the Interplex behave identically provided that the main, i.e., high data rate, high power channel utilizes bi-phase modulation.

The effect of a hard limiter in one arm of the Costas demodulator used for carrier tracking and data recovery of a quadriphase signal was also investigated. It was determined that the hard limiter, although increasing the carrier tracking range of the high power channel, may cause channel ambiguity in which the outputs of the two independent streams reverse. In other words, the low power channel data appears at the channel originally intended for the output of the high power data. This reversal may take place in addition to the normal 0 or 180 degrees data polarity ambiguity associated with the Costas loop demodulator. It is therefore recommended that, if a limiter is used within a Costas loop, amplitude sensing should be employed to correct the channel reversal.

The case of simultaneous multiplexing of three data streams was also reconsidered using a phase multiplexing technique similar to the Interplex. The technique considered consisted of superimposing the two lower rate data channels on an RF carrier which is orthogonal to the bi-phase modulated RF carrier used for the transmission of the main, high data rate signals. The basic modulator and demodulator for this technique are shown in Figure 19. The intermodulation analysis of this quasi-quadriphase modulation technique indicated that for small modulation angles, i.e., less

(a) Three-Channel PM Multiplexer/Modulator

ORIGINAL PAGE IS
OF POOR QUALITY

(b) Costas Loop Three-Channel PSK Demodulato

$$B_1 \gg B_2 \gg B_3$$

Figure 19. Three-Channel PSK Modulator/Demodulator

than ±15 degrees total for the two low rate data channels, the quasi-quadriphase technique is virtually identical to Interplex.

The conclusion was therefore reached that, within certain modulation limits, the quadriphase and Interplex techniques are equivalent from the standpoint of data crosstalk. The main difference between the two techniques is that of implementation. Interplex techniques combine all data signals at baseband and then applies them to a linear phase modulator which operates on only one carrier. Quadriphase techniques require two orthogonal carriers which, after modulation, are combined to provide a composite carrier. Thus, the selection of either technique depends on the system implementation chosen for any specific case.
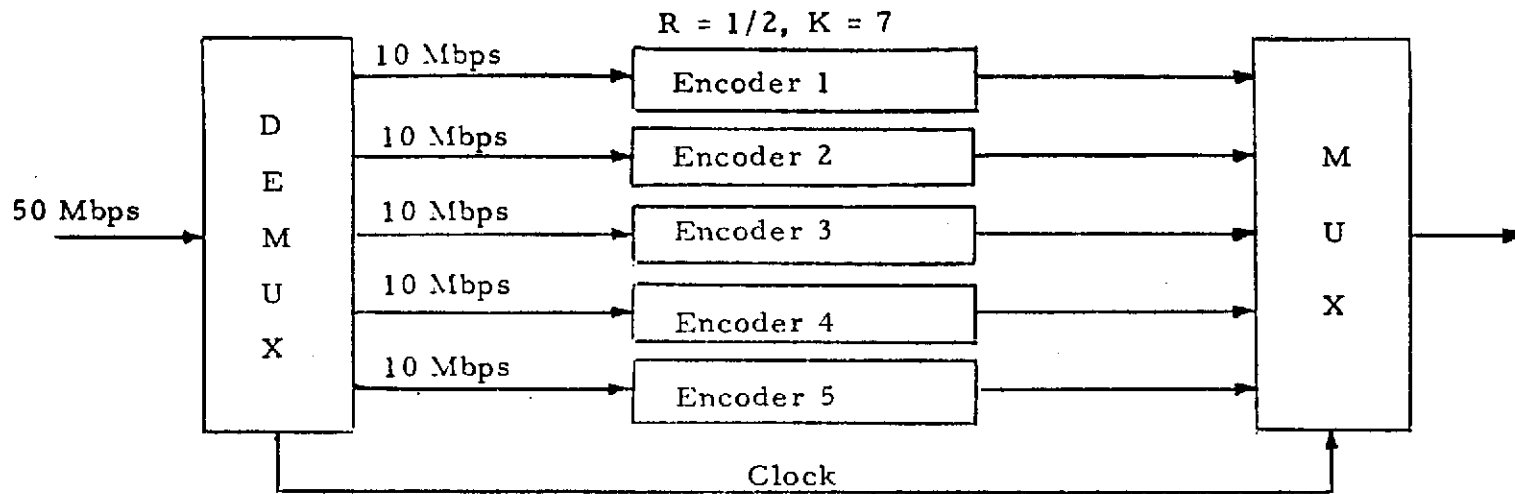
6.3 Convolutional Encoding and Viterbi Decoding at 50 Mbps

6.3.1 Introduction

Convolutional coding for the 50 Mbps Ku-band channel presents an interesting problem because no 50 Mbps Viterbi decoders have been built. For the baseline code ($R = 1/2$, $K = 7$), 10 Mbps Viterbi decoders have been built. Thus, an implementation can be envisioned which uses five encoders and five decoders with some appropriate multiplexers and demultiplexers in between, as shown in Figure 20. This section looks at some alternatives to this implementation. Specifically, it discusses how the encoder portion of Figure 20 can be done with one 31-stage shift register and no mux/demux units. Also, it shows how a conventional 7-stage encoder operating at 50 Mbps can be used with a wide variety of decoder implementations.

6.3.2 Alternate 50 Mbps Coding Strategies

The encoder shown in Figure 20 consists of five 10 Mbps encoders in parallel being fed by the demultiplexed 50 Mbps data stream. Another implementation is to use a 31-stage shift register encoder operating at 50 Mbps, as shown in Figure 21. The tap or connection polynomials $G_1(x)$ and $G_2(x)$ for the 31-stage encoder are related to the tap polynomials $g_1(x)$ and $g_2(x)$ for the 7-stage encoder by $G_1(x) = g_1(x^5)$ and $G_2(x) = g_2(x^5)$. The first two symbols at the output of the long encoder correspond to the first

ORBITER 50 MBPS ENCODER
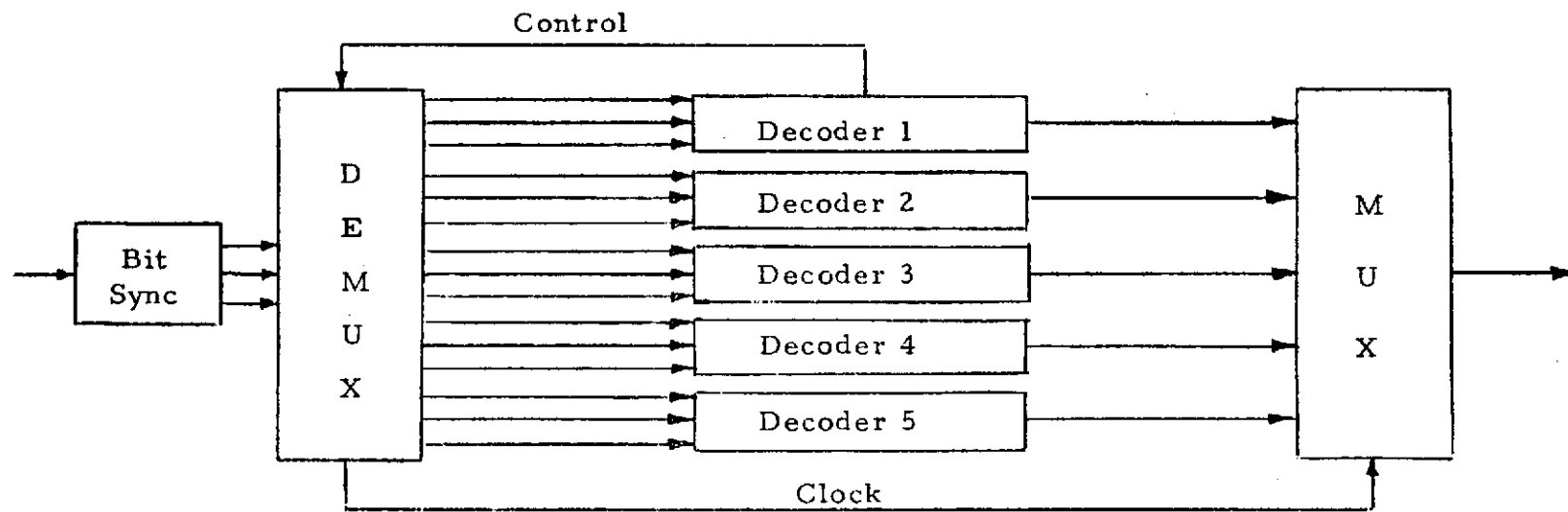
GROUND 50 MBPS DECODER

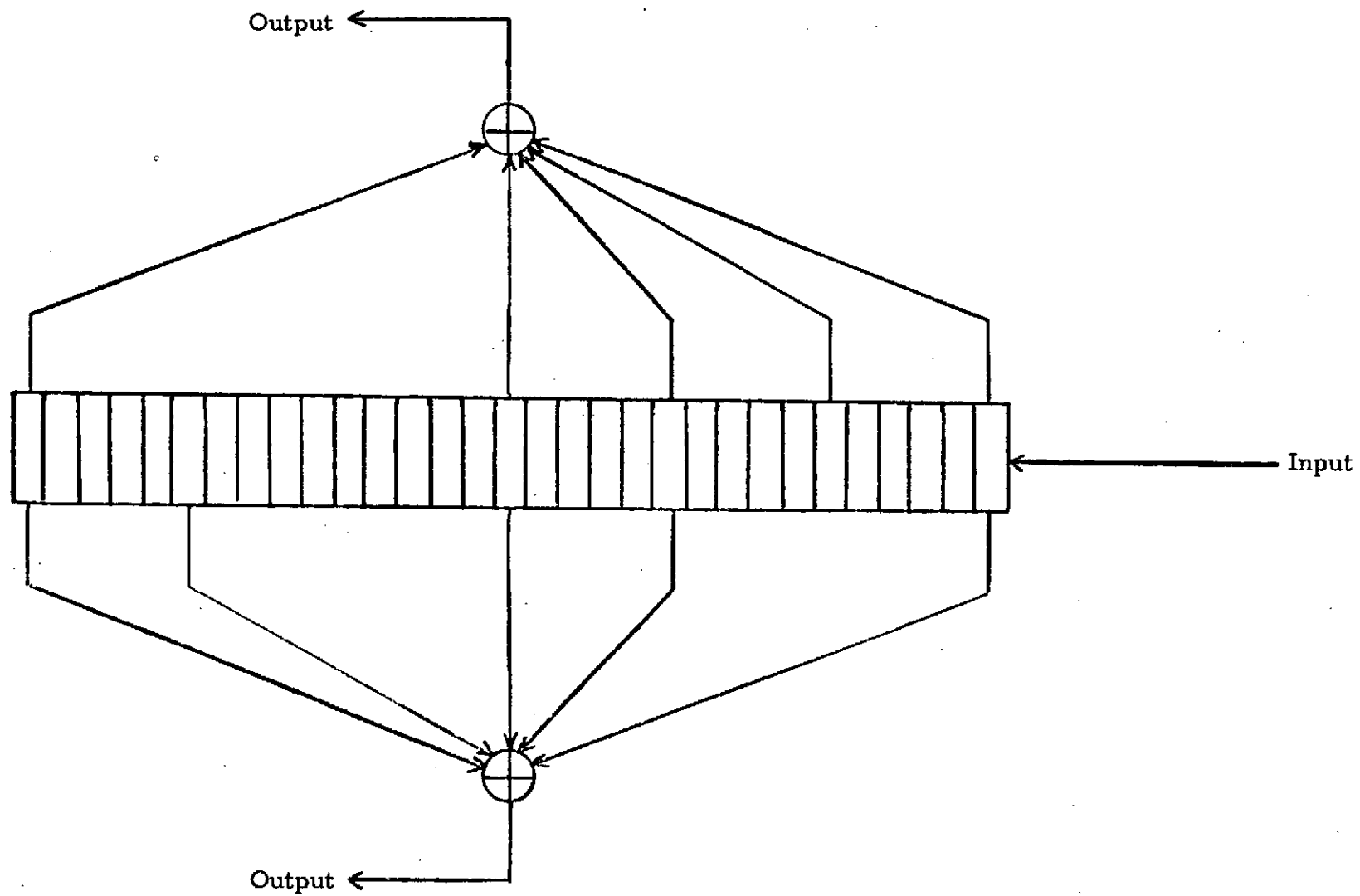Figure 20. Convolutional Encoding and Viterbi Decoding at 50 Mbps

Figure 21. Alternate Encoder for Figure 20

to the first code branch of the first short encoder; the second two symbols correspond to the first code branch of the second short encoder, etc. Note that if this encoder is implemented, it must be decoded by the five parallel Viterbi decoders or by a 50 Mbps sequential decoder, if available.

Now suppose that a 25 Mbps Viterbi decoder is developed. Then only two of these decoders are needed for 50 Mbps. The encoder can either be two 25 Mbps 7-stage encoders in parallel or one 50 Mbps 13-stage encoder with tap polynomials given by $G_1'(x) = g_1(x^2)$ and $G_2'(x) = g_2(x^2)$.

A normal 7-stage encoder operating at 50 Mbps could be used in the Orbiter with any number of decoders at the ground station if the data is blocked. This means that a number of information bits, say 100, is encoded and blocked by finishing off with six additional data 0's. These six zero bits are called the tail, and their purpose is to bring the encoder (also the decoder) back to the all-zero state. These extra bits correspond to 0.25 dB loss in E_b/N_0; of course, this loss can be decreased by increasing the block length. The received data blocks are distributed between the decoders. For example, if five 10 Mbps decoders were used at the ground station, then the data blocks are buffered at the input rate of 50 Mbps and distributed to each decoder at a 10 Mbps rate. Thus, by varying the buffer organization from no buffer for a single 50 Mbps decoder to five or more data block buffers, any number of Viterbi decoders can be used, thereby lowering the effective data rate at each decoder.

In conclusion, some alternatives to the Figure 20 implementation have been presented. The five parallel 10 Mbps decoders can be used with any of three encoder implementation. Similarly, there are three encoders for two parallel 25 Mbps decoders. But for a 50 Mbps decoder, only one encoder, the conventional 7-stage encoder, may be used. On the other hand, the 7-stage encoder can operate with any of three decoder implementations.

7.0   AREAS FOR FURTHER STUDY

During the course of the contract, a number of problem areas were identified which require further study. These areas are summarized below.

7.1   Spread Spectrum Acquisition and Tracking

Both the S-band and Ku-band may have to utilize direct sequence PSK spectrum spreading to minimize the spectral density of the forward link signals impinging upon the Earth. As is generally the case, the acquisition or synchronization time must be minimized. There exist techniques which speed up the time taken for the acquisition. One such technique is sequential detection. The performance of this technique depends on the signal-to-noise ratio at acquisition, the required probability of sync detection and the maximum time allowed for search. The exact tradeoffs between these factors require further consideration to optimize the acquisition performance for both the Ku-band and S-band spread spectrum links.

For the Ku-band link, the encoding of the forward link may increase the data spectrum width to the same order of magnitude as that of spread spectrum. This presents a rather unique situation which requires special consideration.

Once the PN code acquisition is established, the code tracking commences. Code tracking can be accomplished by such techniques as early-late gate tracking or tau-jitter loop tracking. Both techniques have their advantages and disadvantages. Generally, the early-late gate tracking shows better theoretical performance, but its implementation may be more complex than that of the tau-jitter loop. Thus, further consideration has to be given to the tradeoffs involved between these techniques with particular emphasis on the Shuttle spread spectrum link parameters.

7.2   Three-Channel Data Multiplexing Techniques

Preliminary considerations have been given to the various techniques for multiplexing on a single carrier of three data streams, each having different data rates and clocks. This specifically applies to the Ku-band

return link. It was shown that, at least in principle, Interplex and related quadriphase techniques can be used for phase multiplexing of three data channels. The effects imposed by implementation configurations, however, require further study to define the practical limitations of the three-channel data multiplexing techniques considered so far. Alternate techniques such as asynchronous time and/or frequency multiplexing may also be considered. Also, acquisition methods and their peculiarities, such as possible false locks and related phenomena, must be investigated for the various three-channel multiplexing techniques.

7.3 MFSK Coding

Further work should be done in the design of 8-ary FSK convolutional coding, particularly in the transmitter/receiver implementation. Both orthogonal and nonorthogonal signals should be considered, with optimum frequency deviations and receiver bandwidths being determined. An important aspect is the signal design for a bandlimited channel. A new modulation technique, quadrature phase frequency shift keying (QFSK), should be looked at for possible bandwidth conservation.

7.4 System Acquisition Characteristics

The acquisition characteristics of the digital transmission system for communications either directly from the ground or via TDRS to the Orbiter need to be determined. The analysis of carrier, symbol sync, Viterbi decoder branch sync, and multiplexer frame sync acquisition needs to be refined to accurately predict the total system acquisition time as a function of the received signal-to-noise ratio. Effects such as antenna switching on system acquisition should be investigated. A basic set of acquisition techniques and procedures needs to be developed for both direct and TDRS links. In particular, the mutual acquisition of the Orbiter and TDRS high gain antennas must be studied.

7.5 Modulation-Coding Interface Characteristics

Sources of performance degradation on the Viterbi decoder due to the PSK demodulation and bit sync need to be identified. Also, the types

of AGC need to be compared and the effects that the AGC has on the system performance need to be investigated. The interface between the receiver PSK demodulator and the digital signal processor needs to be carefully analyzed to minimize the signal processor performance degradation.

REFERENCES

1. B. D. Trumpis, "Burst Error Correction for the Space Shuttle Command Channels," Axiomatix Report No. R7410-1 (under NASA Contract No. NAS 9-13467), October 2, 1974.

2. B. D. Trumpis, "Addendum to Burst Error Correction for the Space Shuttle Command Channels," Axiomatix Report No. R7501-1 (under NASA Contract No. NAS 9-13467), January 11, 1975.

3. W. C. Lindsey, "Optimum Performance of Costas Type Receivers," Axiomatix Report No. R7410-7 (under NASA Contract No. NAS 9-13467), October 11, 1974.

4. W. C. Lindsey, "Design and Performance of Costas Receivers Containing Bandpass Limiters," Axiomatix Report No. R7502-2 (under NASA Contract No. NAS 9-13467), February 17, 1975.

5. S. Udalov, "Experimental Techniques for Measuring Low Level Spectral Components of Microwave Signals," Axiomatix Report No. R7410-6 (under NASA Contract No. NAS 9-13467), October 11, 1974.

6. S. Udalov, "Feasibility Study of an Interplex Modulation System for the Orbiter's Ku-Band Link," Axiomatix Report No. R7410-5 (under NASA Contract No. NAS 9-13467), October 7, 1974.

7. S. Udalov, "Multiplexing Modulation Formats for the Orbiter's Ku-Band Return Link," Axiomatix Report No. R7502-1 (under NASA Contract No. NAS 9-13467), February 13, 1975.

8. G. K. Huth, "Viterbi Decoder Performance and Complexity," Axiomatix Report No. R7401-1 (under NASA Contract No. NAS 9-13467), January 23, 1974.

9. G. K. Huth, "Command Channel Coding for Shuttle Communications," Axiomatix Report No. R7307-1 (under NASA Contract No. NAS 9-13467), July 20, 1973. Also, G. K. Huth and B. H. Batson, "A Command Encoding Scheme for a Multiplexed Space Communication Link," NTC '73 Conference Record, Atlanta, Georgia, November 26-28, 1973.